arXiv:astro-ph/9610122v1 16 Oct 1996

Physical Properties of 90 AU to 250 AU Pre-Main-Sequence Binaries[*]

Wolfgang Brandner[1] and **Hans Zinnecker**[2]

[1] Astronomisches Institut der Universität Würzburg, Am Hubland, D–97074 Würzburg, Germany
brandner@astro.uni-wuerzburg.de
[2] Astrophysikalisches Institut Potsdam, An der Sternwarte 16, D–14882 Potsdam, Germany
hzinnecker@aip.de

Abstract. We have analyzed photometric and spectroscopic data of a sample of 14 spatially resolved pre-main-sequence binaries (separations $0\rlap{.}''6$ to $1\rlap{.}''7$) in the nearby (150 pc) low-mass star–forming regions of Chamaeleon, Lupus, and ρ Ophiuchi. The spectroscopic data have been obtained with the ESO New Technology Telescope (NTT) at La Silla under subarcsec seeing conditions. All binaries (originally unresolved) were identified as pre-main-sequence stars based on their strong Hα emission — which classifies them as classical T Tauri stars — and their association with dark clouds. One of the presumed binaries turned out to be a likely chance projection with the "primary" showing neither Hα emission nor Li absorption.

Using the spectral A index (as defined by Kirkpatrick et al. 1991), which measures the strength of the CaH band at 697.5nm relative to the nearby continuum, as a luminosity class indicator, we could show that the classical T Tauri stars in our sample tend to be close to luminosity class V.

Eight out of the 14 pairs could be placed on an H–R diagram. A comparison with theoretical pre-main-sequence evolutionary tracks yields that for *all* pairs the individual components appear to be coeval within the observational errors. This finding is similar to Hartigan et al. (1994) who detected that two third of the wider pairs with separations from 400 AU to 6000 AU are coeval. However, unlike Hartigan et al. for the wider pairs, we find no non-coeval pairs among our sample. Thus, the formation mechanism for a significant fraction of the wider pre-main-sequence binaries might be different from that of closer pre-main-sequence binaries. All of the latter appear to have formed simultaneously.

Key words: Stars: Binaries, Pre-Main-Sequence – T association: Chamaeleon, Lupus, ρ Ophiuchi

1. Introduction

In a study entitled "Are wide pre-main-sequence binaries coeval?" Hartigan, Strom & Strom (1994) investigated young T Tauri binary stars with separations $\geq$ 400 AU in order to find clues on how binaries form. A comparison with theoretical pre-main-sequence evolutionary tracks showed that 2/3 of the 26 binaries in their sample are coeval. Thus these binaries very likely formed through fragmentation shortly before or during the collapse phase of a molecular cloud, a process discussed, e.g., by Larson (1978), Boss (1988), Bodenheimer et al. (1988), and Pringle (1989). In the other 1/3 of the cases, however, the secondary appears to be considerably younger than the primary.

Our study aimed at expanding the investigation towards closer pre-main-sequence (PMS) binaries. Close binaries sample a different regime, because for smaller separations circumstellar disks in binaries might be strongly disturbed by the presence of the companion (Papaloizou & Pringle 1977; Artymowicz & Lubow 1994). Thus, the PMS components of a close binary evolve not independently from each other due to disk mediated interaction.

We have analyzed photometric and spectroscopic data of a sample of 14 spatially resolved PMS binaries (separations $0\rlap{.}''6$ to $1\rlap{.}''7$, which corresponds to 90 AU to 250 AU at an average distance of 150 pc) in the nearby low-mass star–forming regions of Chamaeleon, Lupus, and ρ Ophiuchi. The stars had been originally identified as T Tauri stars based on their strong Hα emission and their association with dark clouds by Schwartz (1977, desig. "Sz") and Wilking et al. (1987, desig. "WSB"), and were later on resolved as binaries by Brandner (1992) and Reipurth & Zinnecker (1993).

2. Observations and data reduction

Spatially resolved VRI photometry and optical (600 nm to 720 nm) spectroscopy were obtained at the European Southern Observatory, La Silla, with a CCD camera attached to the Danish 1.54m telescope and with EMMI (ESO Multi Mode Instrument) at the 3.5m New Technology Telescope. All observations were carried out under subarcsec ($\leq 0\rlap{.}''8$) seeing con-
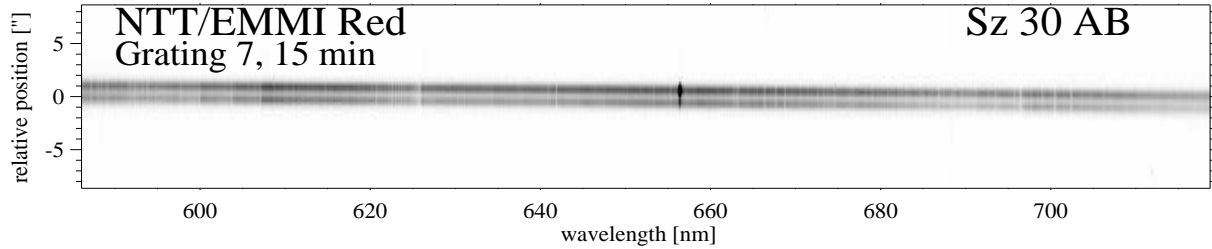

Fig. 1. 2D long-slit spectrum of the pre-main-sequence binary Sz 30 obtained with EMMI at the ESO New Technology Telescope. The strong Hα emission lines of both components are clearly visible.
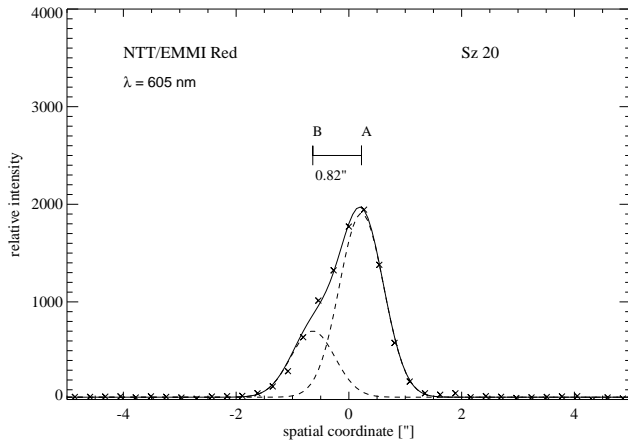

Fig. 2. 1D cut in spatial direction of the 2D long-slit spectrum of Sz 20. The observed intensity distribution is indicated by crosses. Two Gaussian (dashed lines) were fitted in order to model the intensity distribution (solid line).

Table 2. Spectroscopic Observations with NTT/EMMI

designation	alias	λ_c	t_{exp}	sep.	region
ESO Hα281		660 nm	15 min	1″7	Cha I
Sz 20	VV Cha	660 nm	15 min	0″82	Cha I
Sz 24	VW Cha	660 nm	10 min	0″69	Cha I
Sz 30 AB		660 nm	15 min	1″1	Cha I
Sz 48		660 nm	30 min	1″5	Cha II
Sz 59	BK Cha	660 nm	15 min	0″78	Cha II
Sz 62		656 nm	15 min	1″14	Cha II
(20.3.1994)					
Sz 88	HO Lup	645 nm	15 min	1″5	Lup 3
Sz 88	HO Lup	415 nm	30 min	1″5	Lup 3
Sz 101		645 nm	20 min	0″78	Lup 3
Sz 116		645 nm	10 min	1″5	Lup 3
Sz 119		645 nm	15 min	0″59	Lup 3
WSB 18		645 nm	15 min	1″09	ρ Oph
WSB 19		645 nm	15 min	1″5	ρ Oph
WSB 26		645 nm	30 min	1″17	ρ Oph
(17.5.1994)					

Table 1. Photometric observations with the Danish 1.54m telescope/CCD camera (2.3.1995)

object	exposure time (VRI)
Sz 20	3×(10s,10s,10s)
Sz 24	3×(10s,10s,10s)
Sz 30	3×(10s,10s,10s)
Sz 48	3×(30s,20s,20s)
Sz 59	3×(10s,10s,10s)
Sz 62	3×(10s,10s,10s)
WSB 18	3×(30s,20s,—)
WSB 19	3×(10s,10s,10s)
WSB 26	3×(30s,20s,20s)

ditions. The logs of the observations are given in Tables 1 & 2.

The data reduction was carried out using IDL, IRAF, and a stand-alone version of GaussFit (Jeffrys et al. 1991). As the spectra and images of the binary components were blended, we had to apply special techniques in order to deblend the observed intensity distributions. Fitting models using least-squares-fit methods proved to produce more stable and reliable results than using highly non-linear deconvolution techniques.

Figure 1 shows as an example the 2D long-slit spectrum of the 1″1 PMS binary star Sz 30. The slit had been oriented along the direction of both components. While the peaks of the intensity distributions for both components are separated, the wings overlap. For even closer binaries the peaks are no longer resolved. This is clearly visible in Figure 2, which gives a 1D cut in spatial direction of the long-slit spectrum of the 0″82 binary Sz 20 (crosses). In order to separate the intensity distribution of the spectra of the binary components using IDL we fitted a simple model consisting of two Gaussians (Figure 2, dashed lines) to each 1D cut in spatial direction of the 2D spectra. The resulting resolved spectra of the components of Sz 24 and Sz 30 are shown in Figure 3. The spectra of both components of the 0″69 binary Sz 24 are now clearly separated. Note that the emission lines of OI636.2nm, HeI667.9nm, and HeI706.6nm are present only in the spectrum of the primary. Sz 30 is a visual triple system with the tertiary separated by 4″5 from the primary. The tertiary was not included in the present survey. The typical error in the spectra of the secondaries of the closest binaries amounts to 10%.
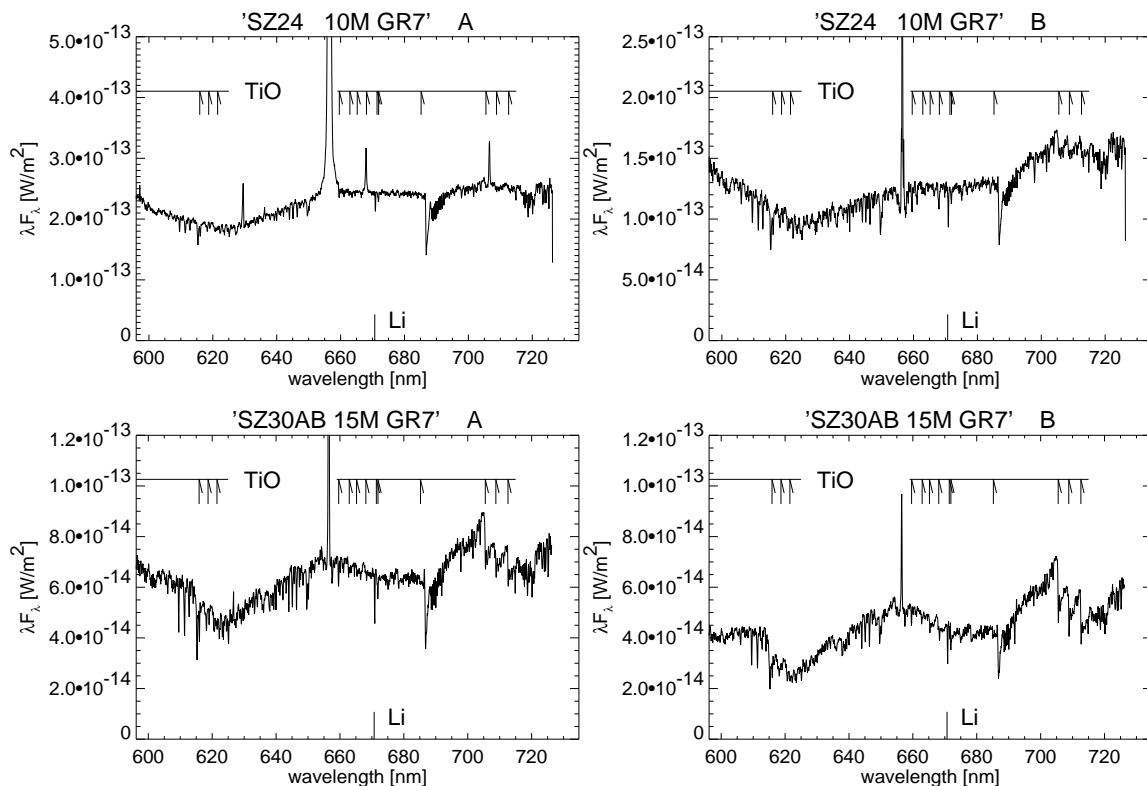
Fig. 3. Resolved spectra of Sz 24 (VW Cha, sep. 0.″69) and Sz 30 (sep. 1.″1). All binary components show Lithium absorption at 670.7 nm. For Sz 24, the OI636.2nm, HeI667.9nm, and HeI706.6nm emission lines are present only in the primary.

Table 3. Comparison of derived spectral types for the binary components with literature values for the unresolved binaries.

name	spectral type		(BZ97)
VV Cha	M1 (MB80)	M1.5 (AJK83)	M1.5 & M3
VW Cha	K5 (R80)	K2 (AJK83)	K5/K7 & K7
Sz 30		M0 (H93)	M0.5 & M2
Sz 48		M0.5 (H^{2}92)	K7/M0 & M0
Sz 59	M0 (H93)	K7–M0 (H^{2}92)	K5/K7 & M0.5
Sz 62	M1 (GS92)	M2 (H^{2}92)	M2 & M3.5
HO Lup		M1 (H^{2}K^{2}94)	K7/M0 & M2
Sz 101		M4 (H^{2}K^{2}94)	M2.5 & M3.5
Sz 116		M1.5 (H^{2}K^{2}94)	M1 & M3
Sz 119		M4 (H^{2}K^{2}94)	M2 & M4

References: AJK83 – Appenzeller et al. (1983), BZ97 – this paper, GS92 – Gauvin & Strom (1992), H93 – Hartigan (1993), H^{2}92 – Hughes & Hartigan (1992), H^{2}K^{2}94 – Hughes et al. (1994), MB80 – Mundt & Bastian (1980), R80 – Rydgren (1980)

For the photometric data we first modeled the local point spread function using field stars and then applied this model to the observed intensity distribution of the binaries using Gauss-Fit for the fitting.

The flux calibration was carried out within IRAF by comparison with photometric and spectro-photometric standard stars[1].

3. Luminosities and effective temperatures and the uncertainties involved

We used the spectral catalogues by Turnshek et al. (1985) and Allen & Strom (1995) in order to determine the spectral types. As spectral features like the TiO band in late-type stars are changing rapidly with spectral type, the determination of the spectral types should be more accurate than half a subclass. Thus, the typical errors in the effective temperature are less than 30K. Table 3 compares the spectral types derived by us for the binary components with those found in the literature for the unresolved binaries. In general there is a good agreement. Only the early spectral classification of VV Cha and VW Cha by Appenzeller (1977 & 1979) was off by one spectral class due to the veiling of weak photospheric lines in the blue part of the spectra which had been used for spectral classification.

The spectral A index (ratio of the continuum flux at 703.5 nm to the flux in the CaH band at 697.5 nm) for most of our binary components is close to that of dwarf stars (c.f. Kirkpatrick

---

[1] The results of the photometric reduction and the reduced spectra of the binary components are available from the author upon request.
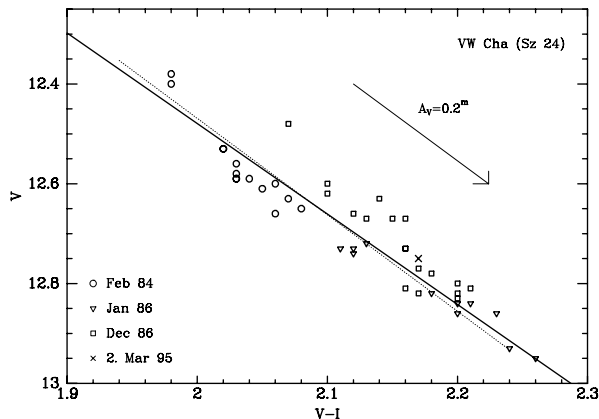
Fig. 4. Colour-magnitude-diagram for Sz 24 (VW Cha) after Bouvier et al. (1988). The different symbols indicate different observing runs. The cross indicates our measurement. The solid line represents a linear fit to the data, the dotted line is a parallel to the extinction vector.

Table 4. Comparison of values derived for the visual extinction A_V of the binary components with literature values for the unresolved binaries

name	A	B	literature	ref.
VV Cha (Sz 20)	$0\overset{m}{.}43\pm0\overset{m}{.}07$	$0\overset{m}{.}67\pm0\overset{m}{.}23$	$1\overset{m}{.}01$	GS92
VW Cha (Sz 24)	$1\overset{m}{.}37\pm0\overset{m}{.}23$	$1\overset{m}{.}26\pm0\overset{m}{.}58$	$2\overset{m}{.}39$	GS92
Sz 30	$0\overset{m}{.}58\pm0\overset{m}{.}04$	$0\overset{m}{.}19\pm0\overset{m}{.}07$	$1\overset{m}{.}18$	GS92
Sz 48	$3\overset{m}{.}41\pm0\overset{m}{.}06$	$3\overset{m}{.}58\pm0\overset{m}{.}10$	$4\overset{m}{.}22$	H^{2}92
Sz 59	$2\overset{m}{.}24\pm0\overset{m}{.}08$	$1\overset{m}{.}60\pm0\overset{m}{.}24$	$2\overset{m}{.}46$	H^{2}92
Sz 62	$1\overset{m}{.}08\pm0\overset{m}{.}04$	$1\overset{m}{.}58\pm0\overset{m}{.}11$	$1\overset{m}{.}54$	H^{2}92

References: GS92 – Gauvin & Strom 1992, H^{2}92 – Hughes & Hartigan 1992

et al. 1991). In general, due to veiling the A index would also be closer to that of dwarf stars and hence could affect a better agreement than there actually is. For a moderate veiling, however, the effect is small and can be neglected for all M-type stars. Thus, the surface gravity of the T Tauri stars in our sample is close to the surface gravity of main-sequence stars and significantly higher than the surface gravity of giants. Walter et al. (1994) tried to derive the intrinsic (R-I) and (V-K) colours of weak-line T Tauri stars by iteratively interpolating between the intrinsic colours of giants and of main-sequence stars. Due to the intrinsic IR excesses of classical T Tauri stars, this method cannot be applied to our sample. Interestingly, Walter et al. (1994) derived intrinsic (R-I) colours for T Tauri stars *bluer* than those of main-sequence stars. On the other hand, synthetic colours computed from atmospheric models of M dwarfs by Allard & Hauschildt (1995) predict *redder* intrinsic colours for stars with a somewhat lower surface gravity than main-sequence stars (Allard, priv. comm.). Thus, at the moment it seems appropriate to assume colours and spectral type–effective temperature relations of main-sequence stars for our sample of PMS stars. We used the compilation provided by Hartigan et al. (1994). They thoroughly discussed various sources of errors and uncertainties in estimating luminosities and effective temperatures for PMS binary components and concluded that variability of the stars is the main source of error.

For VW Cha (Sz 24), the brightest star in our sample, more than 300 photometric measurements are available in the literature, half of them in the Bessell/Cousins broad-band photometric system. These measurements yield a variability of VW Cha from V=$12\overset{m}{.}3$ to $13\overset{m}{.}0$. A colour-magnitude-diagram based on 43 measurements by Bouvier et al. (1988) indicates that the variability is conform with variable extinction (Figure 4). Variable extinction has been proposed by Grinin (1992) as one possible source for the variability observed in many young stars. It might explain the majority of the photometric variability between 500 nm and 1 μm. In this wavelength region, the largest contribution to the overall spectral energy distribution (SED) usually is from the the stellar photosphere (Bertout et al. 1988; Kenyon & Hartman 1990). On the other hand, among extreme CTTS veiling dominates the SED even at these wavelenghts. For extreme CTTS a similar trend of V vs. V-I may be caused by variations in the veiling (a stronger veiling makes the star appear bluer and brighter). In the blue (U, B band) for almost all T Tauri stars the hot boundary layer, hot spots on the stellar surface, and/or photospheric light scattered by circumstellar material contribute more to the overall SED. Hence, the observed variability in U and B cannot be explained by variable extinction alone.

The scatter of $0\overset{m}{.}05$ in brightness of the unresolved binary VW Cha around the linear fit in Figure 4 corresponds to a scatter of $0\overset{m}{.}035$ per component, which is considerably less than the scatter of $0\overset{m}{.}17$ assumed by Hartigan et al. (1994) to be typical for T Tauri stars in the H band.

Assuming that variable extinction is the main course of variability for all stars in our sample the uncertainty in the relative photometry of the components in each binary is the largest source of error in estimating the stellar luminosity. It amounts to up to $0\overset{m}{.}2$ in V for the companion of Sz 24, the binary with the closest separation ($0\overset{''}{.}69$) for which we were able to obtain spatially resolved photometry. In general, however, the errors are considerably smaller ($0\overset{m}{.}05$). We note that this has not to be true for some extreme T Tauri stars like AA Tau, where variations of 1 mag are believed to occur due to hot star spots (Hartigan et al. 1991). The uncertainties resulting from the relative photometry of the binary components are correlated: a fainter secondary means a brighter primary and vice versa.

The highly uncertain distance estimates for the T Tauri stars pose another problem. For Chamaeleon I, e.g., the distance estimates given in the literature range from 115 pc (Thé et al. 1986) to 220 pc (Gauvin & Strom 1992). Similar discrepancies in the distance estimates exist for Chamaeleon II and ρ Ophiuchi. In the following we adopt for Chamaeleon I and ρ Oph a distance of 150 pc. For Chamaeleon II a distance of 200 pc will be assumed (Hughes & Hartigan 1992) as a distance as small as 150 pc would not be conform with the high Lithium abundance observed in the components of Sz 49 and Sz 59 (see

Table 5. Physical properties of the close binary components. Masses and ages are derived from PMS evolutionary tracks by D'Antona & Mazzitelli (1994) based on opacities by Alexander et al. (1989) and the Canuto & Mazzitelli (1990) description of convection.

| | ESO Hα 281 | | Sz 20 | | Sz 24 | | Sz 30 | | Sz 48 | | Sz 59 | |
	A	B	A	B	A	B	A	B	A	B	A	B
separation	1″7		0″82		0″69		1″10		1″5		0″78	
SpT	M0.5	M4.5	M1.5	M3	K5/K7	K7	M0.5	M2	K7/M0	M0	K5/K7	M0.5
T_{eff} [K]	3730	3085	3570	3335	4185	4045	3730	3490	3925	3820	4185	3730
A index	1.04	1.24	1.15	1.26	1.02	1.09	1.10	1.15	1.10	1.09	1.02	1.10
A_V [mag]			0.43	0.67	1.37	1.23	0.58	0.19	3.41	3.58	2.24	1.60
L_{bol} [$L_\odot$]			0.092	0.076	0.61	0.49	0.23	0.16	0.096	0.063	0.16	0.074
age [yr]			$6\cdot10^6$	$3\cdot10^6$	$2\cdot10^6$	$2\cdot10^6$	$2\cdot10^6$	$2\cdot10^6$	$1\cdot10^7$	$1.5\cdot10^7$	$1\cdot10^7$	$9\cdot10^6$
M [$M_\odot$]			0.35	0.20	0.70	0.60	0.48	0.30	0.65	0.56	0.78	0.40
M_B/M_A			0.57		0.86		0.63		0.86		0.51	
$E_{H\alpha}$ [nm]	0.11	-2.3	-9.4	-1.1	-7.9	-0.48	-1.1	-0.26	-1.4	-3.9	-5.4	-2.9
E_{LiI} [pm]	—	27	43	74	26	59	62	75	75	64	43	72
lg N_{LiI}	—	?	-9.0?	-8.8?	-9.4	-8.6	-8.4	-8.5?	-7.9	-8.3	-9.0	-8.2

| | Sz 62 | | Sz 88 | | Sz 101 | | Sz 116 | | Sz 119 | | WSB 18 | |
	A	B	A	B	A	B	A	B	A	B	A	B
separation	1″14		1″5		0″78		1″5		0″59		1″09	
SpT	M2	M3.5	K7/M0	M2	M2.5	M3.5	M1	M3	M2	M4	M2	M2.5
T_{eff} [K]	3490	3255	3925	3490	3415	3255	3645	3335	3490	3170	3490	3415
A index	1.17	1.30	1.08	1.28	1.30	1.19	1.17	1.32	1.22	1.32	1.30	1.22
A_V [mag]	1.08	1.58									4.04	3.41
L_{bol} [$L_\odot$]	0.12	0.074									0.16	0.062
age [a]	$1.5\cdot10^6$	$1.5\cdot10^6$									$2\cdot10^6$	$5\cdot10^6$
M [$M_\odot$]	0.29	0.16									0.30	0.24
M_B/M_A	0.55										0.80	
$E_{H\alpha}$ [nm]	-26.4	-7.0	<-13	-3.4	-0.93	-4.4	-0.41	-0.48	-0.41	-0.46	-0.84	-14.0
E_{LiI} [pm]	50	68	29	68	85	10	45	29	69	170	75	28
lg N_{LiI}	-9.0?	-8.8?	-9.7	-8.5-8.4?	-8.4?	?	-9.0?	?	-8.6?	-7.9??	?	?

| | WSB 19 | | WSB 26 | |
	A	B	A	B
separation	1″5		1″17	
SpT	M3	M3.5	M0	M3
T_{eff} [K]	3335	3255	3820	3335
A index	1.24	1.30	1.14	1.23
A_V [mag]	1.81	2.18		
L_{bol} [$L_\odot$]	0.095	0.061		
age [a]	$2.5\cdot10^6$	$3\cdot10^6$		
M [$M_\odot$]	0.20	0.16		
M_B/M_A	0.80			
$E_{H\alpha}$ [nm]	-5.6	-3.7	-10.9	-17.8
E_{LiI} [pm]	110	61	24	12
lg N_{LiI}	-8.2?	-8.8?	-9.8?	?

below). As both components of a binary star are at the same distance, the error in the absolute distance estimate does not affect the ratio between the estimated luminosities of the two binary components.

As Figure 4 suggests, extinction values might be variable. Therefore estimates of the extinction derived at different epochs cannot be compared directly. Interestingly, the values derived by us are lower than the values quoted in the literature for all stars. *The presence of the secondary causes the unresolved binary to appear redder than the primary actually is and therefore leads to an overestimate of the line of sight extinction*. On the other hand, neglecting excess emission due to veiling leads to an underestimate of the foreground extinction (Hartigan et al. 1991). Therefore, the next step will be to determine the typical veiling for the individual components of all the binaries in our sample.

4. Physical properties: Age, mass, equivalent width, visual extinction, Lithium abundance

Table 5 summarizes the physical properties of the binary components. In Figure 5 we have placed those binary components
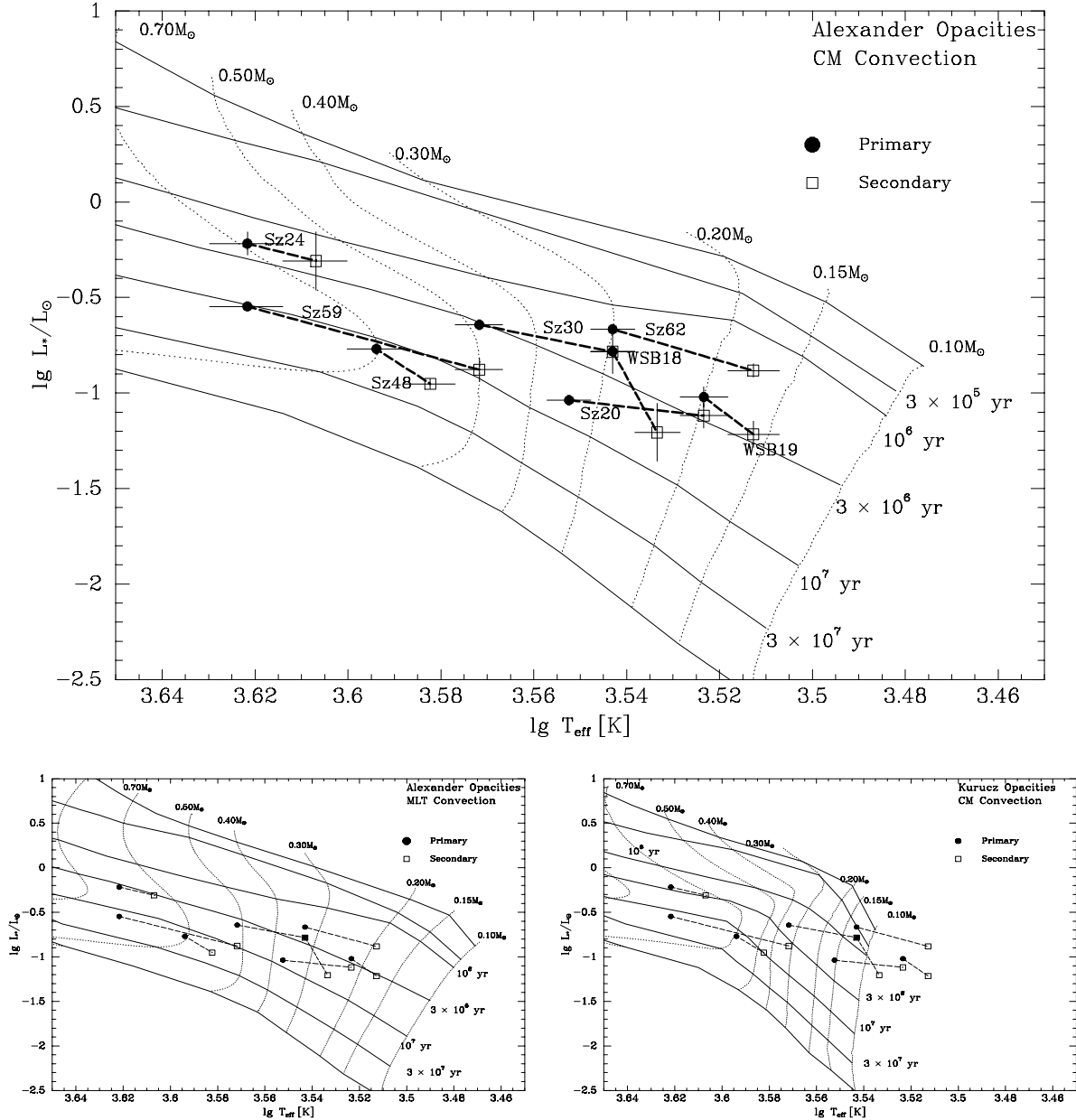
Fig. 5. Binary components placed on an H-R diagram. For comparison theoretical pre-main-sequence evolutionary tracks from D'Antona & Mazzitelli (1994) are overplotted (top). Tracks based on mixing length theory for a description of the convection can only be distinct from those based on the Canuto & Mazzitelli description by a determination of the dynamical masses of pre-main-sequence binaries (bottom left). Tracks based on the opacities from Kurucz (1991) do not provide an adequate description for late-type stars because of the lack of molecular opacities (bottom right).

in H-R diagrams for which we could derive both spatially resolved photometry and spectroscopy. For comparison we show theoretical pre-main-sequence evolutionary tracks from D'Antona & Mazzitelli (1994). These tracks are based on low-temperature opacities from Alexander et al. (1989) or Kurucz (1991) and on the convection model by Canuto & Mazzitelli (1990) or mixing-length theory. The errors in the placement of the individual binary components are indicated. The theoreti-

cal tracks allow us to determine the age and mass of the stars. All of our binaries have mass ratios between 0.5 and 1 (cf. Table 5) whereas only 60% of the binaries studied by Hartigan et al. (1994) have mass ratios in that range. Hence our sample appears to be biased somewhat towards equal mass pairs. However, even among the 15 binaries with mass ratios between 0.5 and 1 in the Hartigan et al. (1994) sample only eleven (75%) are coeval.
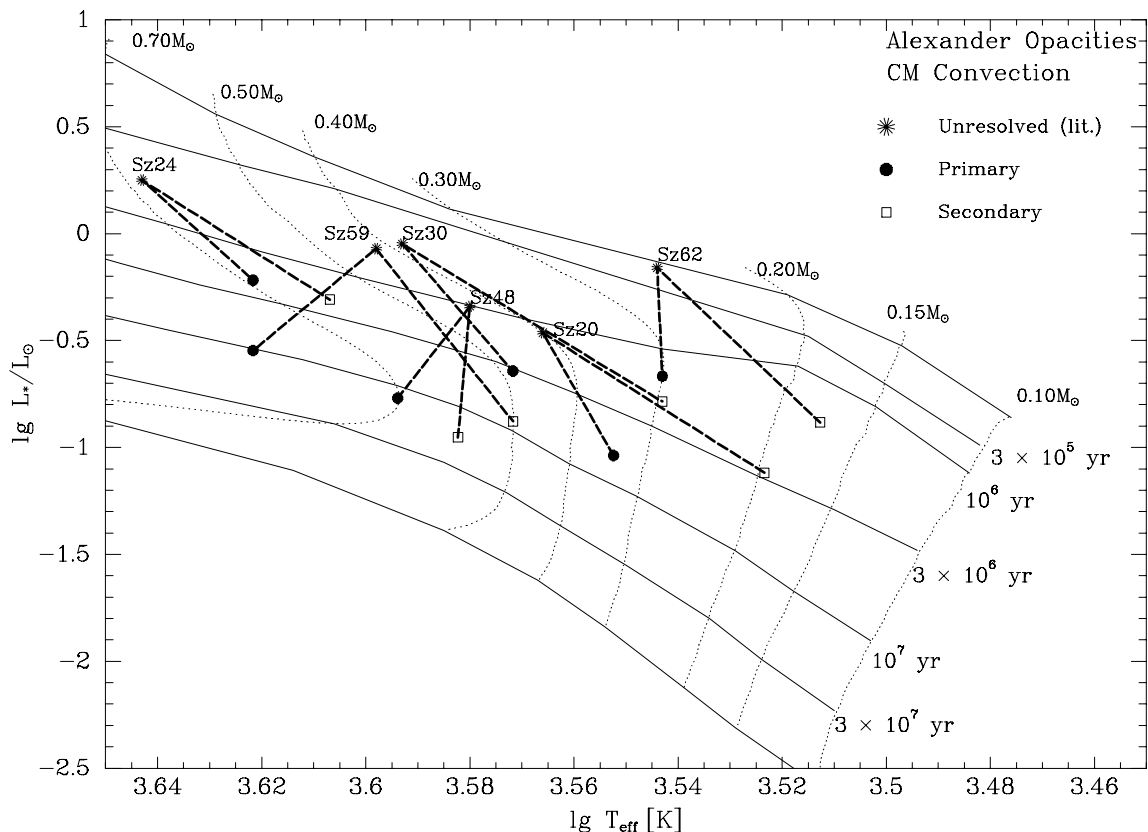
Fig. 6. Unresolved binaries lead to an underestimate of the age of a T Tauri star population. We compare recent literature values for the unresolved binaries (Feigelson et al. 1993, Hughes & Hartigan 1992) with our results for the individual binary components.

Sets of theoretical PMS evolutionary tracks based on different input physics are shown in Figure 5, bottom. A different convection model (i.e. mixing length theory) affects mainly the effective temperature of the evolutionary tracks (and hence the mass estimates) for stars around 0.5 $M_\odot$ to 0.7 $M_\odot$. In the near future dynamical mass determinations for PMS binaries will allow us to distinguish observationally between these two sets of tracks. Tracks based on opacities from Kurucz (1991) lack molecular opacities and hence provide no adequate description for young late-type stars.

Hartigan et al. (1994) compared their observations also to tracks by Swenson et al. (unpublished). Applying the Swenson tracks to our sample of PMS binaries yield masses above 0.4$M_\odot$ and ages between $3 \cdot 10^6$ yr and $3 \cdot 10^7$ yr for the binary components. These ages appear to be rather high given the fact that the stars in our sample are still associated with the molecular clouds (e.g. cf. Brandner et al. 1996; Fig. 5 & 6). On the other hand, observations of the spectroscopic binary NTT 155913-2233 suggest that the tracks by Swenson et al. might provide a better description for PMS stars in a mass range between 0.6$M_\odot$ and 1.1$M_\odot$ than the tracks by D'Antona & Mazzitelli (Prato & Simon, priv. comm.).

Figure 6 nicely illustrates how age and mass estimates can be wrong due to unresolved binaries. For the objects studied in Chamaeleon I and II we have plotted both the most recent literature values for effective temperature and luminosity for the unresolved binaries (Feigelson et al. 1993; Hughes & Hartigan 1992) and the effective temperatures and luminosities as derived by us for the individual binary components. The literature values given by Feigelson et al. (1993) have been scaled to a distance of 150 pc. Note that the somewhat smaller values for the visual extinction towards the binaries derived by us lead also to somewhat lower estimates for the system luminosity in comparison to Feigelson et al. (1993) and Hughes & Hartigan (1992).

Unresolved PMS binaries could lead to a gross underestimate of the age of the stars involved (cf. Ghez 1994) and also induce errors in the individual mass estimates and hence in the derivation of the initial mass function.

In Figure 7 different physical parameters of the primary and secondary are plotted against each other. Fig. 7a (top left) shows the equivalent width of the Hα emission line of the primary and the secondary. No clear correlation exists. Hence, *chromospheric activity and/or accretion rates of primary and secondary appear not to be related*. There are a number of binaries in which only the secondary exhibits strong Hα emission but not the primary. Such stars have only been detected in Hα objective prism surveys because they are binaries and have
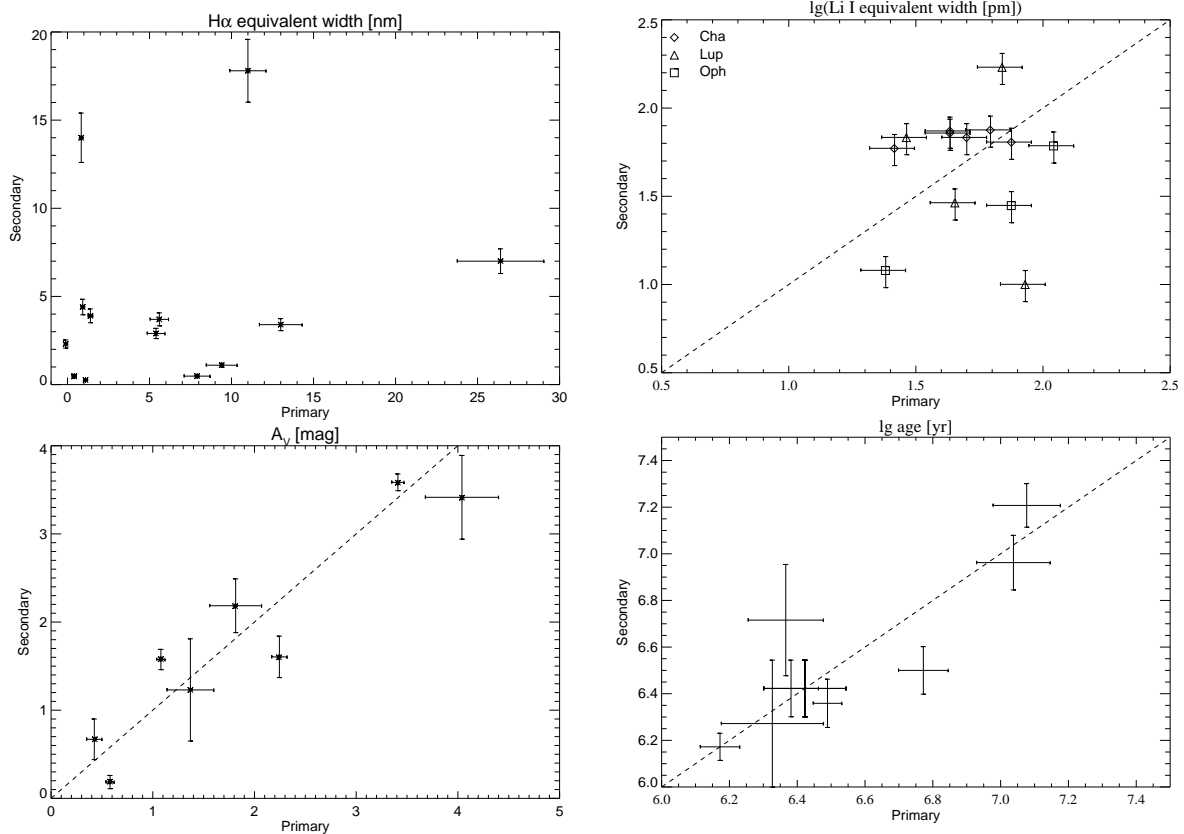
Fig. 7. Correlation of physical parameters of primaries and secondaries: a) Hα equivalent widths, which are a measure of the accretion rate appear not to be correlated. b) Lithium I equivalent widths are also not correlated. c) A_V: The visual extinction towards the primary and towards the secondary of each individual binary show a good correlation. d) Age: All binaries appear to be coeval within the statistical errors.

a secondary bright in Hα. This selection effect may explain at least partially why the number of binaries among pre-main-sequence stars appears to be higher than among main-sequence stars (cf. Ghez et al. 1993; Leinert et al. 1993; Reipurth & Zinnecker 1993).

The Lithium I (670.7nm) equivalent width of primary and secondary (Fig. 7b, top right) are not correlated as a test based on rank statistics indicates. Differences in the individual veiling and the non-linear dependence of the Lithium abundance on age and effective temperature might be responsible for that. See below for a more detailed analysis considering curve of growth calculations and Lithium depletion as a function of age and effective temperature. ESO Hα 281 A is the only star in our sample of 28 binary components which does not show any sign of Lithium absorption. The small value of its A index indicates that ESO Hα 281 A is a background giant.

The visual extinction towards the primary and secondary (Fig. 7c, bottom left) are in good agreement with each other. This indicates that both components of each binary are embedded equally deep in the dark clouds and thus gives further evidence that the objects studied are indeed physical binaries. Furthermore, the agreement of the extinction values yields that the circumstellar disks around the individual components in each binary system in our sample are aligned.
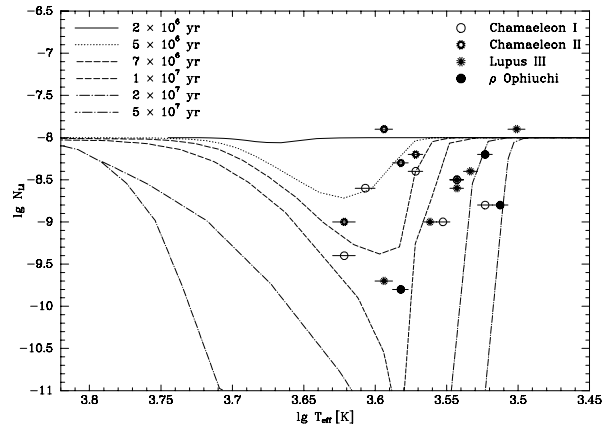

Fig. 8. Lithium abundance as a function of effective temperature. We have also plotted theoretical isochrones from D'Antona & Mazzitelli (1994) based on opacities from Alexander et al. (1989) and the Canuto & Mazzitelli (1991) description of convection.

The age of the primary and secondary (Fig. 7d, bottom right) derived from the theoretical pre-main-sequence evolutionary tracks is generally in good agreement for ages in a

range of a few 10^6 yr to 10^7 yr. Only for one star (Sz 20) the secondary might be somewhat younger than the primary. However, the deviation amounts to only 1.5 σ and thus could very well be a purely statistical fluctuation.

Based on the curve of growth calculations by Martín et al. (1994) we were able to derive Lithium abundances for our sample of pre-main-sequence binary components. Figure 8 shows the Lithium abundances as a function of effective temperature. Overplotted are theoretical isochrones from D'Antona & Mazzitelli (1994). As the curve of growth calculations are based on Kurucz model atmospheres they are only valid down to effective temperatures of about 3700 K. Below that temperature the abundances derived from the model calculations lie probably too low (Martín et al. 1994). Veiling of photospheric lines could additionally lead to an underestimate of the actual Lithium abundance. Hence, the values plotted in Figure 8 merely represent lower limits in most cases.

For the components of Sz 48 and Sz 59 the Lithium isochrones suggest an age of less than 10^7 yr. In order to match this with their positions in the H-R diagram the distance to these stars (and thus towards the Chamaeleon II cloud) has to be at least 200 pc.

5. Summary

We have surveyed 14 binaries with separations between 0.''6 and 1.''7. In 27 of the 28 individual stars we did find Lithium absorption, which (together with their Hα emission and association to dark clouds) classifies them as T Tauri stars. One of the presumed binaries turned out to be a likely chance projection with the "primary" showing neither Hα emission nor Lithium absorption. This object (ESO Hα 281 A) is very likely a background giant. Similarly, Aspin et al. (1994) found the 'companion' to the PMS star ESO Hα 279 A to be a background giant.

A comparison of the equivalent width of the Hα emission line of the primaries and secondaries showed that they are not correlated with each other. Some of the originally unresolved T Tauri stars were only picked up in Hα surveys because they are binaries and have a *secondary* with strong Hα emission whereas the primary shows only weak Hα emission. Therefore, samples of Hα selected T Tauri stars might be biased towards binaries.

Eight out of the 14 pairs could be placed on an H–R diagram. A comparison with theoretical pre-main-sequence evolutionary tracks yields that for *all* pairs the individual components appear to be coeval within the observational errors. This finding is similar to Hartigan et al. (1994) who found that 2/3 of the wider pairs with separations from 400 AU to 6000 AU are coeval. However, unlike Hartigan et al. for the wider pairs, we find no non-coeval pairs among our sample. Thus, young binaries with separations less than 400 AU might indeed represent a different regime as compared to binaries with separations between 400 AU and 6000 AU. Otherwise, it might very well be that the wide non-coeval binaries in the sample from Hartigan et al. are just chance projections and not physically related to each other.

References

Alexander D., Augason G., Johnson H. 1989 ApJ 345, 1014
Allard F., Hauschildt P.H. 1995 ApJ 445, 433
Allen L.E., Strom K.M. 1995 AJ 109, 1379
Appenzeller I. 1977 A&A 61, 21
Appenzeller I. 1979 A&A 71, 305
Appenzeller I., Krautter J., Jankovics I. 1983 A&AS 53, 291
Artymowicz P., Lubow S.H. 1994 ApJ 421, 651
Aspin C., Reipurth B., Lehmann T. 1994 A&A 288, 165
Bertout C., Basri G., Bouvier J. 1988 ApJ 330, 350
Bodenheimer P., Rozyczka M., Yorke H.W., Tohline J.E. 1988 in *Formation and Evolution of Low Mass Stars* p. 139, eds. Dupree A.K. & Lago M.T.V.T.
Boss A.P. 1988 Comments in Astrophys. 12, 169
Bouvier J., Bertout C., Bouchet P. 1988 A&AS 75, 1
Brandner W. 1992 Diploma thesis, Universität Würzburg
Brandner W., Alcalá J.M., Kunkel M., Moneti A., Zinnecker H. 1996 A&A 307, 121
Canuto V., Mazzitelli I. 1990 ApJ 370, 295
D'Antona F., Mazzitelli I. 1994 ApJS 90, 467
Feigelson E.D., Casanova S., Montmerle T., Guibert J. 1993 ApJ 416, 623
Gauvin L.S., Strom K.M. 1992 ApJ 385, 217
Ghez A. 1994 BAAS 185, 99.01
Ghez A., Neugebauer G., Matthews K. 1993 AJ 106, 2005
Grinin V.P. 1992 A&AT 3, 17
Hartigan P. 1993 AJ 105, 1511
Hartigan P., Kenyon S.J., Hartmann L. et al. 1991 ApJ 382, 617
Hartigan P., Strom K.M., Strom S.E. 1994 ApJ 427, 961
Hughes J., Hartigan P. 1992 AJ 104, 680
Hughes J., Hartigan P., Krautter J., Kelemen J. 1994 AJ 108, 1071
Jeffrys W.H., McArthur B., McCartney J.E. 1991 BAAS 23, 997
Kenyon S.J., Hartman L.W. 1990 AJ 99, 869
Kirkpatrick J.D., Kelly D.M., Rieke G.H. et al. 1991 ApJS 77, 417
Kurucz R. 1991 in Crivellari & Hubeny (eds.), NATO ASI Series, p. 441
Larson R.B. 1978 MNRAS 184, 69
Leinert C., Zinnecker H., Weitzel N., et al. 1993 A&A 278, 129
Martín E., Rebolo R., Pavlenko A.M.Y. 1994 A&A 282, 503
Mundt R., Bastian U. 1980 A&AS 39, 245
Papaloizou J.C.B., Pringle J.E. 1977 MNRAS 181, 441
Pringle J.E. 1989 MNRAS 239, 361
Reipurth B., Zinnecker H. 1993 A&A 278, 81
Rydgren A. 1980 AJ 85, 444
Schwartz R.D. 1977 ApJS 35, 161
Thé P., Wesselius P.R., Tjin-A-Djie H.R.E., Steenman H. 1986 A&A 155, 347

Turnshek D.E., Turnshek D.A., Craine E.R., Boeshaar P.C. 1985 Technical Report, Western Research Company, Arizona

Walter F.M., Vrba F.J., Mathieu R.D., Brown A., Myers P.C 1994 AJ 107, 692

Wilking B.A., Schwartz R.D., Blackwell J.H. 1987 AJ 94, 106